2024 SPE Improved Oil Recovery Conference

SPE-218246-MS

Aqueous Ketone Solution for Wettability Alteration in High-salinity-high-temperature Carbonate Reservoirs

Tesleem Lawal, Abouzar Mirzaei-Paiaman, and Ryosuke Okuno

The University of Texas at Austin, Austin, Texas, USA

Abstract

Enhanced oil recovery (EOR) has been studied for high-salinity high-temperature (HSHT) carbonate reservoirs, but their thermodynamic conditions, brine chemistry, and petrophysical properties tend to pose various technical challenges for both gas- and chemical-based EOR. This paper presents an experimental study of aqueous solution of 3-pentanone for EOR in a carbonate reservoir with a brine salinity of 224,358 ppm at a reservoir temperature of 99°C. The short dialkyl ketone was previously studied as a sole additive to injection brine for rapid wettability alteration in oil-wet carbonate rocks without affecting the water/oil interfacial tension; however, it had not been tested under HSHT conditions. The main objective of this research was to investigate the impact of 3-pentanone on convective oil displacement in oil-wet carbonate rocks under HSHT conditions.

First, aqueous stability was confirmed for mixtures of 3-pentanone and two brines: formation brine (FB) with a salinity of 224,358 ppm and injection brine (IB) with a salinity of 54,471 ppm at reservoir temperature. Quantitative proton nuclear magnetic resonance (^{1}H NMR) analysis was used to determine the solubility of 3-pentanone in FB and IB. Spontaneous and forced imbibition experiments were conducted to assess imbibition enhancement in oil-aged Texas Cream carbonate cores by a solution of 3-pentanone in IB (3pIB) and compared with IB. Afterward, corefloods with oil-aged carbonate cores were performed by injecting IB followed by 3pIB as a tertiary flooding scenario and also by injecting only 3pIB as a secondary flooding scenario. Analysis of the spontaneous imbibition and coreflooding results was assisted by history-matched numerical models where capillary pressure and relative permeability curves were obtained. These data were further used to infer wettability alteration potential of 3-pentanone solution. Because of the markedly different solubilities of 3-pentanone in injection brine (1.1 wt%), formation brine (0.3 wt%), and oil (first-contact miscible), material balance analysis of corefloods was performed to understand the transport of 3-pentanone through varying salinities from injection brine (54,471 ppm) and resident brine (224,358 ppm) while being mixed with in-situ oil.

Spontaneous and forced imbibition tests confirmed the wettability alteration of oil-aged carbonate rocks by 1.1-wt% 3pIB. This was further supported by the slope analysis of temporal recovery data as well as analyzing history-matched capillary pressure and relative permeability data. Coreflooding results showed increased oil production rate and reduced residual oil saturation by 3pIB. Relative permeability data, through Lak and modified Lak wettability indices, also indicated a wettability alteration toward more water-wetness by 3-pentanone solution.

1. Introduction

Carbonate reservoirs, which hold more than half of the world's oil reserves, typically show highly heterogeneous properties at different scales with varying wettability states between intermediate- and oil-wet (Lake et al. 2014). Such petrophysical properties tend to make improved oil recovery by waterflooding inefficient at micro and macro scales (Sheng 2013; Al Shalabi et al. 2014). A negative capillary pressure under oil-wet conditions prevents the injected water from spontaneously imbibing into unswept oil-wet regions (Standnes and Austad 2000; Allan and Sun 2003; Manrique et al. 2007). Thus, the injected water ends up bypassing the oil in the oil-wet rock matrices and flowing through fractures and other high-permeability hydraulic paths in carbonate oil reservoirs.

Oil recovery in oil-wet reservoirs can be improved by changing oil-water multiphase flow characteristics by a rock-wettability alteration from oil-wet to water-wet. The wettability alteration of oil-wet porous media to a more water-wet state is expected to promote the spontaneous imbibition of water from water-swept regions into the bypassed regions and to increase the ratio of viscous to capillary forces in the convective displacement of oil by water. Such wettability alteration has been studied using chemicals, such as surfactants, polymers, alkali agents, and a combination of these chemicals. Some of those techniques modify the rock surface properties, but also

reduce oil-water interfacial tension (IFT) (Kathel and Mohanty 2013; Morsy et al. 2013; Alvarez et al. 2018; Lu et al. 2019; Zeng et al. 2018; Gbadamosi et al. 2019). Reducing oil-water IFT tends to adversely affect the spontaneous imbibition process because it lowers the driving capillary forces. The main mechanisms of wettability alteration in surfactant-based enhanced oil recovery (EOR) include ion pair formation, surfactant adsorption, and micellar solubilization (Austad and Milter 1997; Standnes and Austad 2000; Alvarez and Schechter 2016; Burrows et al. 2020).

Surfactant EOR has been extensively studied for depleted oil reservoirs with various petrophysical properties, especially under low-temperature and low-salinity conditions. The literature is much scarcer on surfactant applications under high-salinity and high-temperature (HSHT) reservoir conditions because of implementation challenges; for example, the aqueous/surfactant stability and surface activity tend to diminish under HSHT conditions (Somasundaran and Fuerstenau 1972; Kulkarni and Somasundaran 1976; Ziegler and Handy 1981; Belhaj et al. 2020). Puerto et al. (2012) reported that reservoirs with temperatures from 10 to 120°C are candidates for surfactant flooding, but the effectiveness of surfactants can be damaged during the EOR process. Sheng (2015) indicated that a practical limit is 93°C in reservoir temperature and 100,000 ppm in brine salinity for surfactant EOR. Despite these challenges, new classes of surfactants have been studied and successfully tested for EOR under HSHT conditions (Barnes et al. 2008; Puerto et al. 2012; Chen and Mohanty 2015; Levitt et al. 2016; Alammari et al. 2020).

An alternative method for improved waterflooding has been studied in a series of publications on use of ketone solvent as a sole additive to injection brine (Wang et al. 2019, 2020ab, 2022; Argüelles-Vivas et al. 2020, 2022; Lawal et al. 2022). Argüelles-Vivas et al. (2022) described that 3-pentanone was most suitable as a wettability modifier among the oxygenated solvents tested in their research. 3-Pentanone is a short dialkyl ketone and is miscible with oil and slightly soluble in brine (Wang et al. 2019). It was observed that concentrations of 3-pentanone below the solubility in water did not affect the oil-water IFT (Wang et al. 2019; Alghunaim et al. 2021). Because of the highly asymmetric solubility of 3-pentanone between oil and water (brine), 3-pentanone is expected to rapidly transfer from the injection brine to the resident oil in unswept regions when aqueous solution of 3-pentanone is injected into oil-bearing porous media. Argüelles-Vivas et al. (2020) and Wang et al. (2020, 2021) presented material balance analyses for their dynamic imbibition experiments, in which the injected aqueous solution flowed through artificially fractured cores; that is, spontaneous imbibition was the main mechanism of oil recovery from the matrices surrounding the fracture volume. Their experiments included carbonate cores (Argüelles-Vivas et al. 2020; Wang et al. 2020), like those in this research, as well as tight outcrop cores (Wang et al. 2021).

This paper is concerned with the use of aqueous 3-pentanone solution for EOR in an HSHT carbonate reservoir with a formation-brine salinity of 224,358 ppm at a reservoir temperature of 99°C. Such HSHT conditions were studied in none of the previous studies on 3-pentanone. In addition, two important aspects of this research are as follows: (1) the solubilities of 3-pentanone were markedly different among injection brine (1.1-wt%), resident reservoir brine (0.3-wt%), and oil (miscible), and (2) corefloods with no fractures were studied for the first time in this research. Then, the main objective of the research was to investigate the impact of 3-pentanone and its transient mass transfer on convective oil displacement by coreflooding and on spontaneous imbibition by static soaking experiments. Section 2 presents the materials and methodology. Section 3 details the results and main findings of the Amott wettability tests, coreflooding, and numerical history matching. Section 4 provides a summary of the paper.

2. Materials and Methods

2.1. Fluid Properties.

A dead crude oil sample from an HSHT carbonate reservoir was used for this research. The initial reservoir pressure and temperature are 27.2 MPa (3945 psia) and 99°C, respectively. Table 1 summarizes the properties of the oil sample. The formation brine (FB) (224,358 ppm) and the injection brine (IB) (54,471 ppm) were prepared as presented in Table 2.

Table 1—Properties of the crude oil sample used in this research

Molecular weight (g/mol)		246
Density (g/mL)		0.8688 (at 22°C) 0.8122 (at 99°C)
Viscosity (cp)		11.0 (at 22°C) 2.0 (at 99°C)
SARA (wt%)	Saturates	53.5
	Aromatics	30.4
	Resins	13.4
	Asphaltenes (pentane insoluble)	2.7
Acid number (mg-KOH/g-oil)		0.05

Table 2—Ionic compositions and salinities of the brines used in this research

Ion	Concentration (ppm)	
	FB (pH = 6.35)	IB (pH = 7.53)
Na^+	63402	16710
K^+	——	583
Ca^{2+}	19560	650
Mg^{2+}	2281	2019
Sr^{2+}	——	15
Br^-	——	69
Cl^-	138763	30200
HCO_3^-	25	25
SO_4^{2-}	327	4200
Total dissolved solids	224358	54471

The stability of 3-pentanone in FB (formation brine) and IB (injection brine) was tested at the reservoir temperature of 99°C. No salt precipitation occurred for the 3-pentanone concentrations from 1 to 5-wt%. With no salt precipitation in the equilibrium aqueous phase, a 3-pentanone-rich liquid phase appeared as the 3-pentanone concentration increased above 1-wt% for FB and above 2-wt% for IB. Quantitative proton nuclear magnetic resonance (^{1}H NMR) analysis showed that the solubility of 3-pentanone at 99°C was 0.3-wt% in FB and 1.1-wt% in IB. This marked difference in 3-pentanone solubility between IB and FB could influence the interphase transfer of 3-pentanone near the oil displacement fronts. As in all the previous studies of aqueous 3-pentanone solution, the aqueous phase remained stable below the 3-pentanone solubility at 99°C, making it suitable for use with the FB and IB during injection. The concentration of 3-pentanone in IB was 1.1-wt% in this research, and the solution is referred to as "3pIB."

The IFT values for crude oil/IB and crude oil/FB were measured using a spinning drop tensiometer (KRÜSS Scientific) at 99°C. The IFT was 14.2 mN/m for crude oil and IB, and 21.2 mN/m for crude oil and FB. Wang et al. (2019) and Alghunaim et al. (2021) previously showed that 3-pentanone does not change the IFT between oil and brine at low 3-pentanone concentrations (0.8 – 1.1-wt%); therefore, the IFT was not measured for the 3-pentanone solutions and oil in this research.

2.2. Core Properties and Preparation.

Four Texas Cream limestone outcrop core plugs were used in the experiments. The mineralogy of the Texas Cream Limestone cores was determined using X-ray diffraction (XRD) analysis as follows: 97.5-wt% calcite, 0.6-wt% dolomite, and 0.9-wt% pyrite.

The core plug was first evacuated for one hour and the effective porosity was determined by saturating it with formation brine (FB). Then, FB was injected at flow rates of 100, 80, and 60 mL/hr at room temperature to determine the permeability from the measured differential pressure. A stable pressure difference was recorded after waiting for 30 minutes at each flow rate. The system was then heated to 99°C, and each FB-saturated core plug underwent crude oil injection using a coreflooding setup. The coreflooding system for saturating the cores consisted of two Teledyne ISCO pressurization pumps, three accumulators for the FB, crude oil, and nitrogen, a Hassler-type core holder, a hydraulic manual pump to apply confining pressure, a back-pressure regulator (BPR), pressure gauges, and an oven. A confining pressure of 6998 kPa and a back pressure of 1482 kPa were used during the oil injection. The crude oil was injected at a constant flow rate of 25 mL/hr. After oil breakthrough, the injection rate was gradually increased to 50 mL/hr to reduce the capillary end effect on phase saturation profile. The crude oil injection continued until negligible FB production. The initial oil and water saturations (S_{oi} and S_{wi}) were estimated based on the produced FB volume. Then, the cores were immersed at 99°C for 12 to 17 days in a heavy oil with an acid number of 8.08 mg-KOH/g-oil (equivalent to a concentration of 0.134 M stearic acid) to accelerate the process of making rock oil-wet. McCaffery and Mungan (1970) showed that stearic acid enhances oil-wetness of calcite surfaces. After aging, the cores were flooded again with the dead crude oil (properties listed in Table 1) using the same coreflooding setup to displace the oil used for aging. Table 3 summarizes the measured petrophysical properties for each core plug. Core plugs #1 and #2 were used for Amott wettability tests, while core plugs #3 and #4 were used for coreflooding experiments.

Table 3—Petrophysical properties of the TX Cream limestone core plugs used in this research

Property	Core Plug #1	Core Plug #2	Core Plug #3	Core Plug #4
Length (cm)	11.6	10.3	11.4	9.81
Diameter (cm)	3.79	3.80	3.79	3.79
Porosity, ϕ	0.311	0.298	0.308	0.306
Permeability, k (mD)	13.0	11.0	11.9	11.8
Pore volume, V_p(mL)	40.7	34.8	39.5	33.9
Initial water saturation, S_{wi}	0.446	0.416	0.450	0.487
Initial oil saturation, S_{oi}	0.554	0.584	0.550	0.513

2.3. Amott Wettability Tests.

Amott wettability tests were performed on core plugs #1 and #2 at 95°C. Amott tests included both spontaneous and forced imbibition experiments. The spontaneous imbibition experiments were performed at a temperature slightly lower than the reservoir temperature to protect the integrity of the Amott cell glassware at very high temperatures. Additionally, the crude oil used to prepare core plugs #1 and #2 were degassed at the test temperature to prevent oil recovery due to solution gas drive during the spontaneous imbibition experiments. Aqueous solutions of IB and 1.1-wt% 3pIB were used for the spontaneous and forced imbibition experiments. The entire preparation was conducted with the solutions and glassware inside the oven at 95°C to minimize any oil recovery from the thermal expansion of fluids during the course of experiments. The recovered oil volume was periodically measured during the experiments. Following completion of the experiment, for the 3pIB case, the concentrations of 3-pentanone in the recovered oleic phase and the aqueous solution were measured using ^{1}H NMR analysis.

The forced imbibition experiment commenced following the completion of the spontaneous imbibition experiment. Before each forced imbibition experiment, the recovered oleic phase from the spontaneous imbibition experiment was transferred to a clean container. Then, the core was removed from the Amott cell, placed inside a core holder, and set up in a coreflooding system as described in Section 2.2. The corresponding aqueous solution (IB or 3pIB) was injected into the core at a constant flow rate of 40 mL/hr. This injection rate was set for a capillary number limit of 2×10^{-5} (Lake et al. 2014). The produced oil volume was periodically measured. Once the water cut became greater than 99%, the injection rate was increased to 120 mL/hr to reduce the capillary end effect. The concentration of 3-pentanone in the recovered oleic phase was measured at different times using proton NMR analysis.

The Amott wettability index to water (I_w) was calculated as the ratio of the oil recovery by spontaneous imbibition to the total oil recovery (i.e., the total oil production achieved in both spontaneous and forced imbibition tests), as shown in Eq. 1.

$$I_w = \frac{oil\ recovery\ by\ spontaneous\ imbibition}{total\ oil\ recovery} \tag{1}$$

The oil recovery histories from the spontaneous imbibition experiments were also studied by a slope analysis technique to infer wettability alteration as proposed by Mirzaei-Paiaman et al. (2013, 2017). When oil recovery (i.e., oil production divided by pore volume) is plotted against the scaling group, Eq. 2, the data within the infinite acting period of imbibition fall on a straight line. For a set of cores, different slopes of the resulting straight lines indicate different wettability states because all the factors influencing the spontaneous imbibition rate are included in the scaling group, except for wettability. The scaling group is

$$\text{Scaling group} = \sqrt{\frac{2\sigma\sqrt{\frac{k}{\phi}}}{(\mu_w + \sqrt{\mu_w\mu_0})L_c^2}}\ \ t^{0.5} \tag{2}$$

where σ is the interfacial tension between water and oil, k is the permeability, ϕ is the porosity, μ_w is the water viscosity, μ_0 is the oil viscosity, and t is the time. L_c is the characteristic length defined as

$$L_c = \sqrt{\frac{V_m}{\sum_{n=1}^{N}\frac{A_{m,n}}{l_{m,n}}}} \tag{3}$$

where N is the number of the core open faces to spontaneous imbibition, V_m is the core bulk volume, A_m is the surface area open to flow in a given flow direction, and l_m the distance from the open surface to the corresponding no-flow boundary.

2.4. Coreflooding Experiments.

Two sets of coreflooding experiments were performed to quantify the performance of 3-pentanone in tertiary and secondary injection modes. Figure 2 shows the experimental setup for both injection modes. The system consisted of a vertically mounted Hassler-type core holder, two Teledyne ISCO pumps, four accumulators for oil, IB, 3pIB, and nitrogen, a hydraulic manual pump to apply confining pressure, a BPR, pressure gauges, and an oven. The confining pressure was set at 6998 kPa and the back pressure was set at 1482 kPa. The back pressure was applied to avoid oil production by the solution gas drive mechanism since the bubble point pressure of the dead oil sample at the tested temperature was around 310 kPa (Figure 1). The effluent samples were collected at 22°C and atmospheric pressure. In the secondary injection mode, the IB accumulator was disconnected from the system as the oil-displacing fluid was only 3pIB.

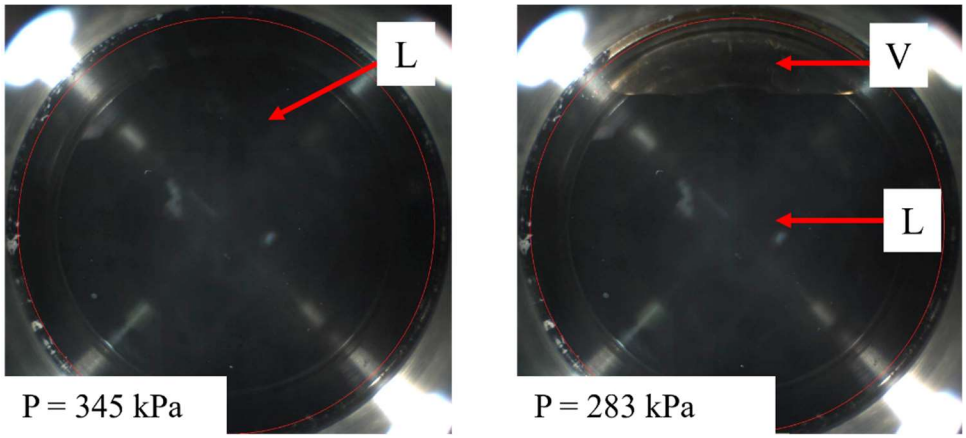

(a) (b)

Figure 1—Photos of the dead crude oil sample in a PVT cell during constant mass expansion experiments at 99°C. (a) Cell pressure is above the bubble point pressure and only a single liquid phase exists (b) Cell pressure is below the bubble point pressure and liquid and vapor phases exist.

The core plugs were prepared as described in Section 2.2 and initial water saturation was established. For the tertiary mode of 3pIB coreflooding, IB was first injected at 5 mL/hr until it established the baseline production where water-cut reached 98%. Then, 3pIB was injected at the same rate until the produced effluent reached 98% water cut (or until no further change in oil level in the produced effluent sample was observed). For the secondary mode of 3pIB coreflooding, after establishing the initial water saturation, 3pIB was injected at 5 mL/hr until 98% water cut was reached.

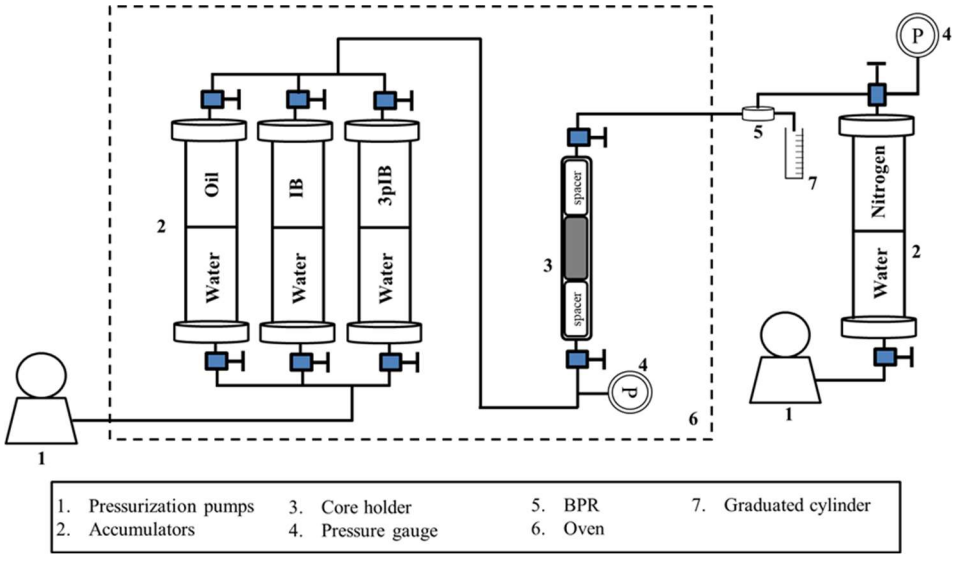

Figure 2—Schematic of coreflooding setup for the tertiary and secondary 3pIB injection.

2.5. Material Balance Analysis.

A material balance analysis was performed for the (pseudo)components: brine, oil, and 3-pentanone to analyze the 1-dimensional coreflooding experiments based on the ideal-mixing assumption. The primary objectives were to determine the fractional amount of

each component (brine or 3-pentanone) that was absorbed into the matrix during the coreflooding process, and the relative contribution of each component to recovering oil from the matrix pore volume. Figure 3 shows a schematic of the material balance for the coreflooding experiments. The positive direction is from the surrounding to the system, which is the core.

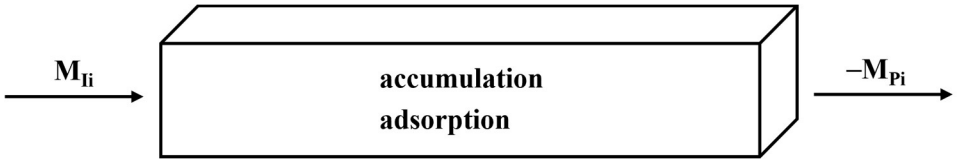

Figure 3—Schematic of the mass balance analysis for coreflooding experiments.

The material balance analysis considered the following assumptions:

1. Ideal mixing between 3-pentanone and oil and between 3-pentanone and water
2. Isothermal pseudo-steady state flow during the experiment
3. 3-Pentanone first adsorbs on the rock surface before accumulating in the matrix pore volume
4. No other chemical reactions, such as mineral dissolution, other than the adsorption of 3-pentanone on the rock surface

For a given time interval, Δt, the accumulation of component i in the matrix pore volume, ΔM_{Ai}, was calculated as shown in Eq. 4.

$$\Delta M_{Ai} = M_{Ii} + M_{Pi} + M_{adsorbed,i} \tag{4}$$

where i is (1 for brine, 2 for oil, and 3 for 3-pentanone), M_{Ii} is the amount of component i going into the system, and M_{Pi} is the amount of component i going into the system (i.e., $-M_{Pi}$ goes out of the system as shown in Figure 3). The amount of component i that accumulates in the system is the accumulated fraction for component i, F_i for Δt; that is,

$$F_i = \frac{M_{Ai}}{M_{Ii}} \tag{5}$$

2.6. History Matching.

The spontaneous imbibition and coreflooding results were history-matched using CMG IMEX (Computer Modeling Group, 2022). The main objectives were to obtain relative permeability and capillary pressure, and to estimate saturation profiles during the displacements. Simulation of the spontaneous imbibition process used a single-porosity simulation approach. The numbers of simulation grid cells in the x, y, and z directions were 32, 32, and 102, respectively. The outer grid cells represented a large-volume fracture system that was initially at 100% water saturation. We assumed zero capillary pressure and linear relative permeability curves in the fracture system. The core was thus modeled as a 30 × 30 × 100 grid cell system. The height and the cross-sectional area of the simulated core were identical to the actual core. The numerical simulation model for spontaneous imbibition experiments was calibrated against the oil production data by adjusting the parameters for relative permeability and capillary pressure.

For the corefloods, the numbers of simulation grid cells in the x, y, and z directions were 100, 1, and 1, respectively. The height and the cross-sectional area of the simulated core were identical to the actual core. The numerical simulation model for coreflooding experiments was calibrated against the oil production data by adjusting the parameters for relative permeability.

The calibrated relative permeability and capillary pressure were used for qualitative assessment of wettability alteration by 3pIB in comparison to IB for the spontaneous imbibition experiments. The relative permeability calibrated using coreflooding data was employed for the same purpose. The calibrated relative permeabilities for the spontaneous imbibition and coreflooding tests inferred wettability quantitatively via Lak and modified Lak wettability indices, which vary from −1 (strongly oil-wet systems) to 1 (strongly water-wet systems). Near-zero values for these indices represent intermediate wettability (Mirzaei-Paiaman, 2021; Mirzaei-Paiaman et al., 2022). Lak wettability index I_L is expressed as

$$I_L = \alpha\left(\frac{0.3 - k_{rw@ROS}}{0.3}\right) + \beta\left(\frac{0.5 - k_{rw@ROS}}{0.5}\right) + \frac{CS - RCS}{1 - S_{or} - S_{wc}} \tag{6}$$

where $k_{rw@ROS}$ is the water relative permeability at residual oil saturation (relative permeability is defined as the effective permeability divided by oil permeability at the interstitial water saturation), CS is the crossover saturation in fraction, S_{or} is the residual oil saturation, S_{wc} is the connate or initial water saturation, and RCS is the reference crossover saturation defined as

$$RCS = \frac{1}{2} + \frac{S_{wc} - S_{or}}{2} \tag{7}$$

Coefficients α and β are determined based on $k_{rw@ROS}$ as follows.

$$If \begin{cases} k_{rw@ROS} < 0.3, then\ \alpha = 0.5, \beta = 0 \\ 0.3 \leq k_{rw@ROS} \leq 0.5, then\ \alpha = \beta = 0 \\ k_{rw@ROS} > 0.5, then\ \alpha = 0, \beta = 0.5 \end{cases} \tag{8}$$

Modified Lak wettability index I_{ML} is given by

$$I_{ML} = \frac{A_o - A_w}{A_o + A_w} \tag{9}$$

where A_o and A_w are respectively the areas below oil and water relative permeability curves.

3. Results and Discussion

3.1. Amott Wettability Tests.

Figure 4 shows the oil recovery, in terms of %OOIP, from the spontaneous imbibition experiments with IB and 1.1-wt% 3pIB at 95°C. The final oil recovery was 24.4% for the IB case and 34.0% for the 3pIB case. For the 3pIB case, the 3-pentanone concentration was 3.15-wt% (8.5 mol%) in the recovered oleic phase and 0.47-wt% (0.44 mol%) in the recovered aqueous phase. Since the concentration of 3-pentanone in the injection brine was 1.1-wt%, the result confirmed the dominant mass transfer of 3p from the aqueous phase to the oleic phase during the experiment.

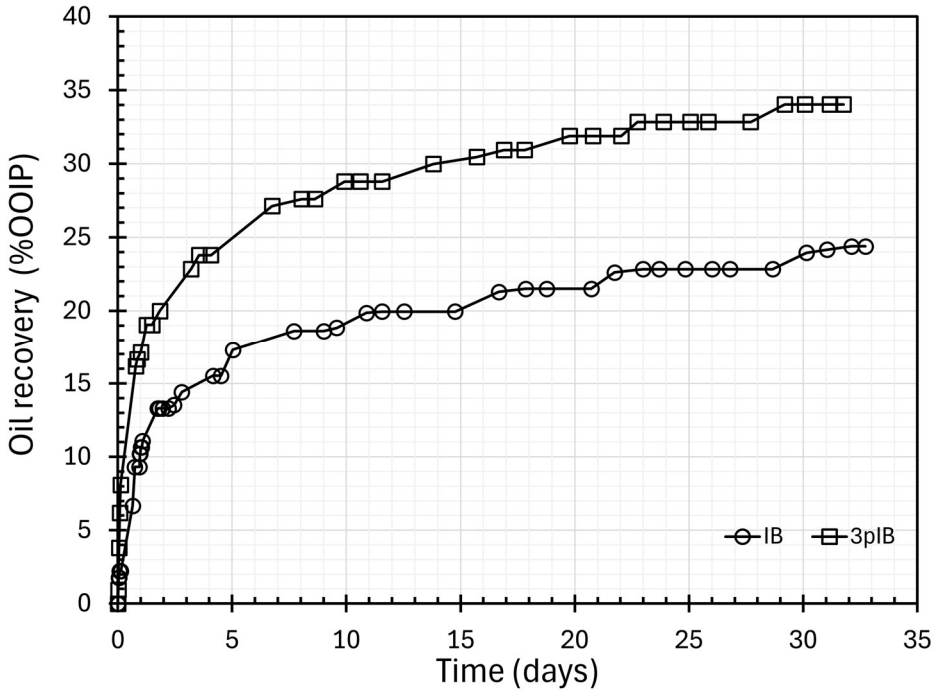

Figure 4—Oil recovery from spontaneous imbibition with IB and 1.1-wt% 3pIB at 95°C.

Figure 5 shows the oil recoveries by the forced imbibition of IB and 1.1-wt% 3pIB. The oil recovery at 0 hydrocarbon pore volumes injected (HCPVI) in this figure is the final oil recovery from the spontaneous imbibition test (Figure 4). The oil recovery by the forced imbibition was 58.9% at 18.5 HCPVI for the IB case and 58.4% at 19.2 HCPVI for the 3pIB case. Therefore, the total oil recovery from the spontaneous and forced imbibition experiments was 83.3% for IB and 92.4% for 3pIB. The 3-pentanone concentration in the produced oil for the 3pIB case was measured to be 2.6-wt% using ^{1}H NMR. This 3-pentanone concentration is an average value across five ^{1}H NMR measurements of produced oil samples with a minimum of 2.33-wt% and a maximum of 2.98-wt%.

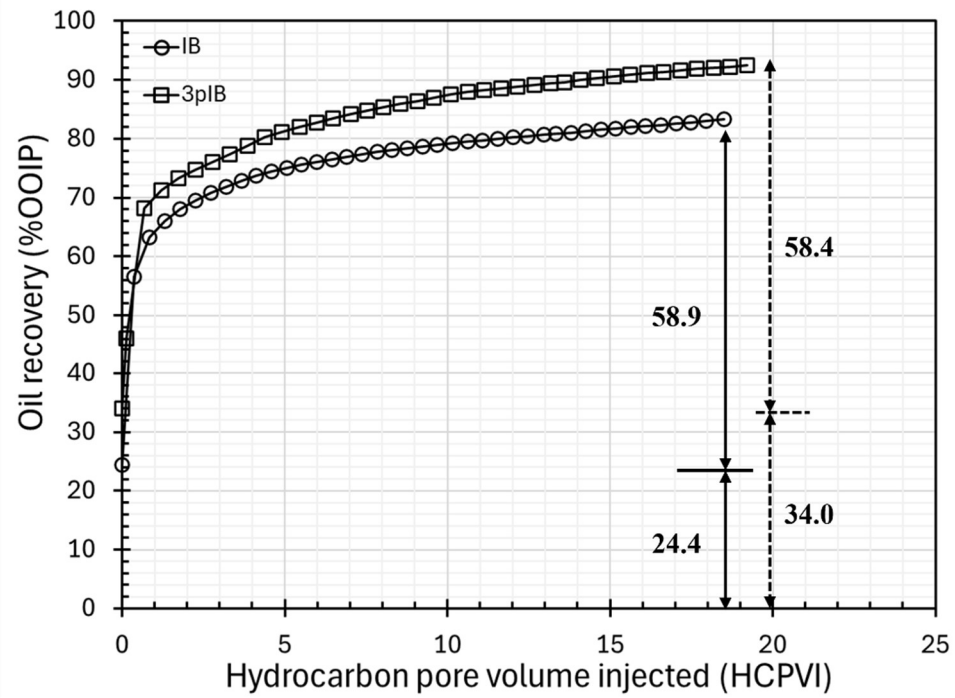

Figure 5—Oil recovery from the spontaneous and forced imbibition experiments with IB and 1.1-wt% 3pIB. The oil recovery at 0 PVI is from the preceding spontaneous imbibition. The Amott indices to water are 0.29 for IB and 0.37 for 3pIB.

The Amott indices to water was calculated to be 0.29 for the IB imbibition and 0.37 for the 3pIB imbibition, indicating wettability alteration towards a more water-wet state by 3pIB. However, the actual Amott index to water for the case of 3pIB is expected to be even greater than 0.37. This is because the oil displacement during the forced imbibition phase was owing to injection of 3pIB where a further wettability alteration was likely to occur. As a result, a greater oil production in the forced imbibition phase lowered the calculated Amott index.

Figure 6 presents the oil recovery against the scaling group (Eq. 2). As previously mentioned, this scaling group considers all the factors influencing the oil recovery except for wettability. Therefore, the difference in the recovery curves is attributed to different wettability states. A more water-wet state in the 3pIB case is evident because of more rapid oil production in this case than in the IB case. Figure 7 presents the same analysis only for the straight portion of the recovery curve. The slopes are 0.056 and 0.034 for the 3pIB and IB cases, respectively, which indicates that 3pIB made the rock more water-wet by a factor of 1.6.

Figure 8 shows the results of the history matching of the spontaneous imbibition experiments. As mentioned earlier, the objective was to make the simulation model match the observed data by changing relative permeability and capillary pressure parameters. The obtained relative permeability and capillary pressure are presented in Figure 9. A clear wettability alteration was observed toward a more water-wet state by 3pIB solution because the 3pIB case yielded a greater positive capillary pressure and also a smaller water relative permeability. The Lak and modified Lak wettability indices were calculated to evaluate the wettability by 3-pentanone during the spontaneous imbibition experiments. The Lak index was 0.03 for the IB case and 0.12 for the 3pIB case, indicating a wettability alteration of the core to a more water-wet state by the 3pIB. The modified Lak index was 0.45 for the IB case and 0.46 for the 3pIB case, indicating a marginal difference in wettability alteration by 3pIB.

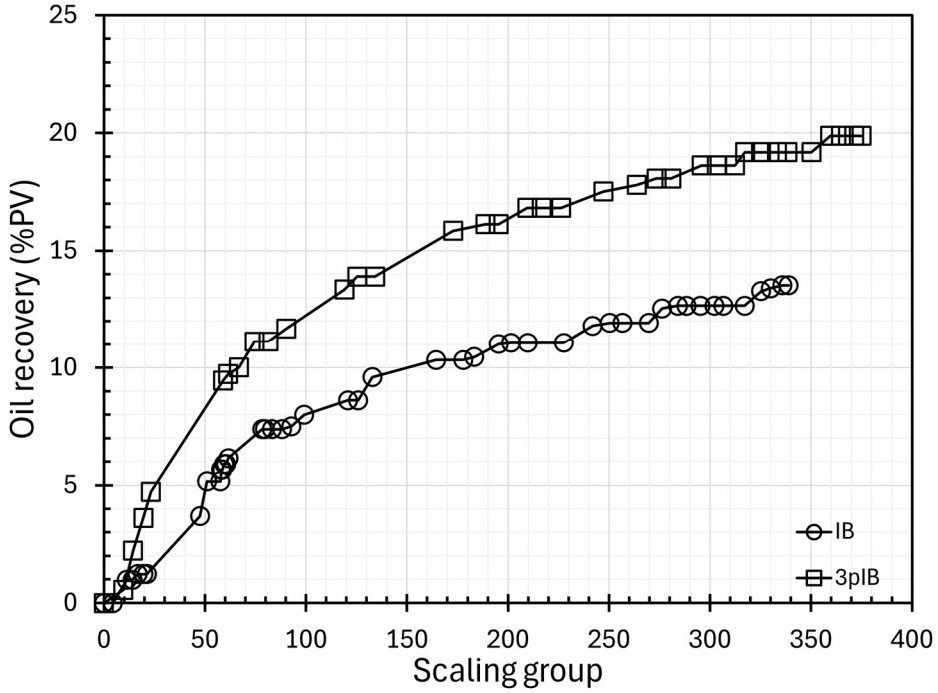

Figure 6—Oil recovery from spontaneous imbibition with IB and 1.1-wt% 3pIB at 95°C.

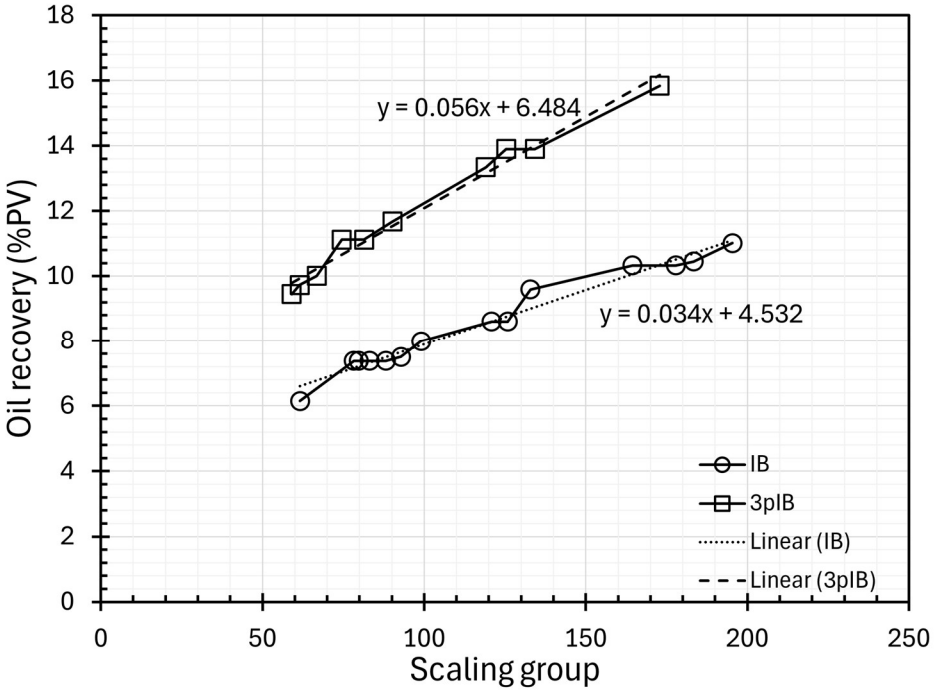

Figure 7—Straight portion of the oil recovery from spontaneous imbibition with IB and 1.1-wt% 3pIB at 95°C.

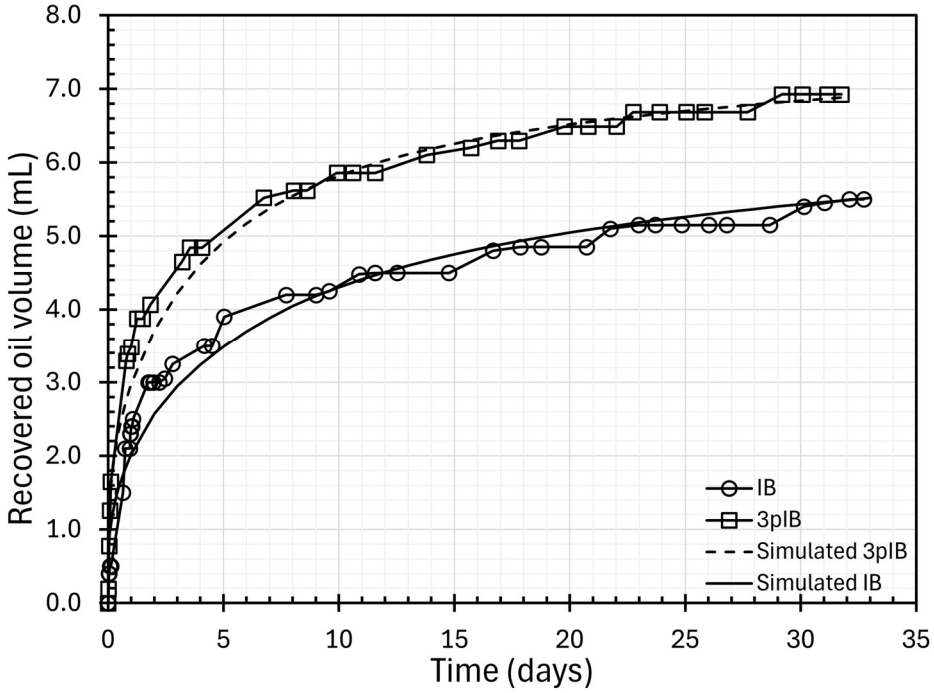

Figure 8—History-matched result of recovered oil volume during spontaneous imbibition of IB and 1.1-wt% 3pIB.

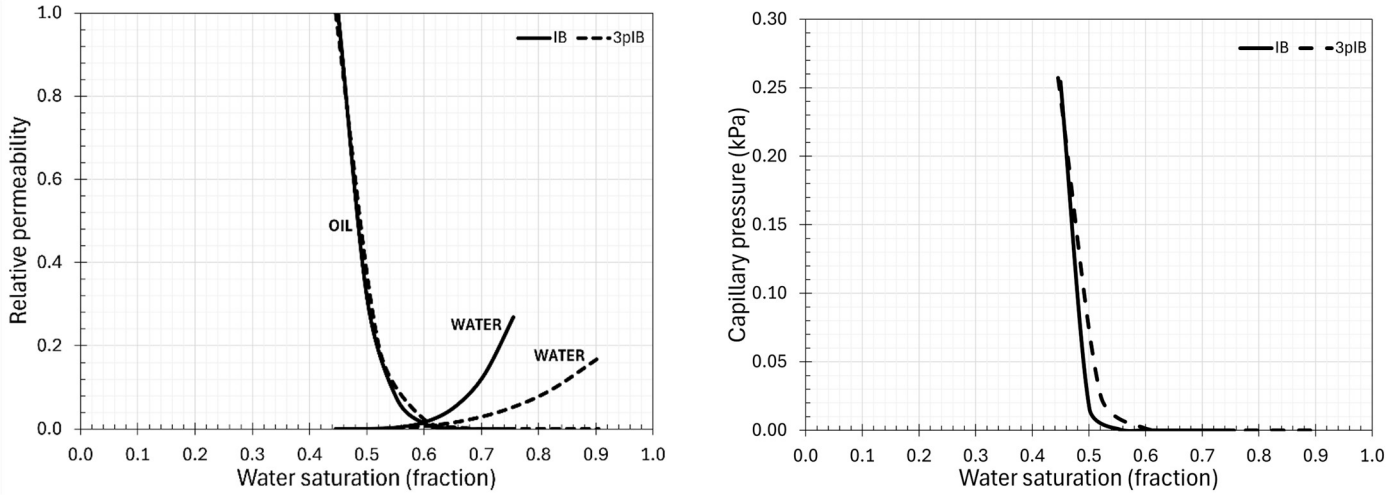

(a) (b)

Figure 9—Adjusted parameters during history matching of the spontaneous imbibition experiments with IB and 1.1-wt% 3pIB (a) relative permeability (b) capillary pressure.

The corresponding water saturation profiles, derived from the simulation model, are shown in Figure 10 for the central vertical cross section of the core plug. For the IB case (Figure 10a), the displacement was predominantly counter-current in the early stage of the imbibition, but it involved both counter- and co-current flow in the late times. This can be explained by inverse Bond number, the ratio of capillary forces to gravity forces. At the early times when water saturation in the core was small, capillary forces were stronger than gravity forces and this led to a capillary dominated counter-current spontaneous imbibition. At late times when water saturation in the core increased, the relative strength of capillary forces respect to gravity forces decreased. This led to a mixed flow regime of counter- and co-current flow, where the co-current flow was caused by the gravity forces. Note that oil recovery in a gravity-dominated system is expected to be slower than in a capillary-dominated system because in the former, oil recovery increases with time whereas in the latter, it increases with the square root of time. In the 3pIB case (Figure 10b), the displacement was always dominantly counter-current. Stronger water-wetness in this case led to the driving capillary forces that were much stronger than gravity forces (i.e., a greater inverse Bond number than that in the IB case).

The following equation estimates the inverse Bond number. Figure 11 shows the inverse Bond number during IB and 3pIB imbibition experiments.

$$B = \frac{P_c(S_w)}{(\rho_w - \rho_o) \times g \times H} \tag{8}$$

where B is the inverse Bond number, P_c is the capillary pressure which is a function of water saturation in core S_w, ρ_w is water density, ρ_o is oil density, g is the gravitational constant, and H is the core height.

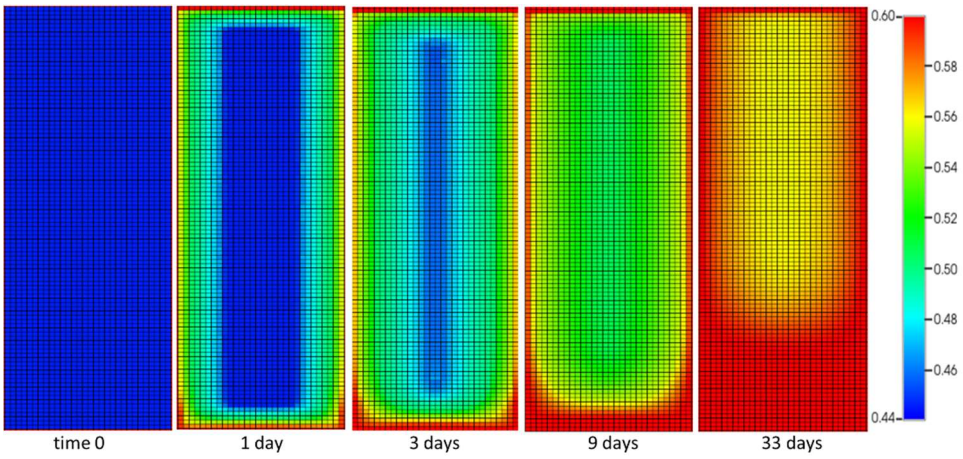

(a)

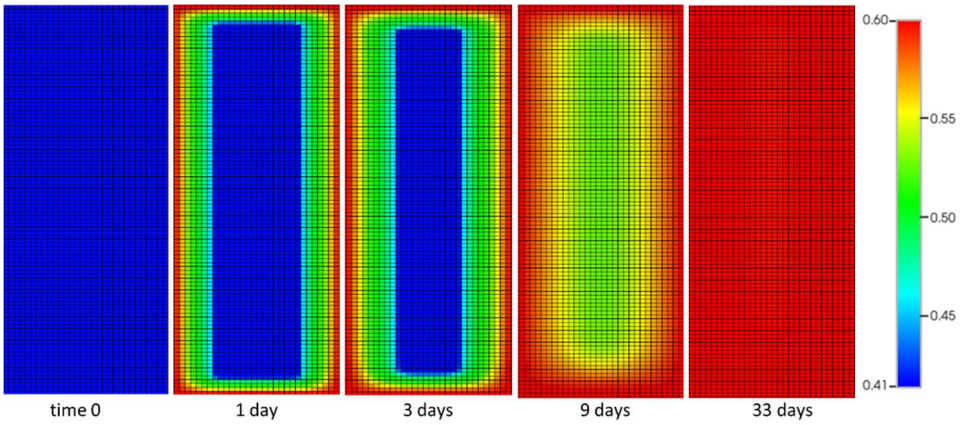

(b)

Figure 10—Simulated water saturation profiles during the spontaneous imbibition of (a) IB and (b) 1.1-wt% 3pIB.

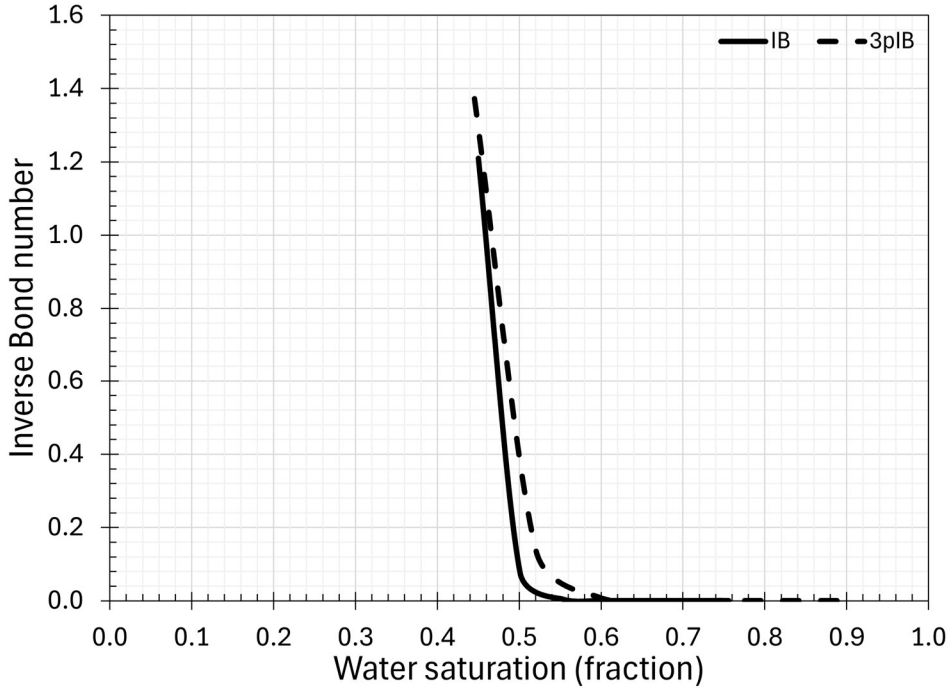

Figure 11—Inverse Bond number during the spontaneous imbibition of IB and 1.1-wt% 3pIB.

3.2. Coreflooding Experiments.

Tertiary 3pIB Injection.

This coreflood was performed to investigate the oil displacement by 3pIB in the tertiary injection mode. After the core preparation as described in Section 2.2, IB was injected for 3.48 HCPV at an injection rate of 5 mL/hr. After the IB established a stable production history, the tertiary 3pIB injection began with the same injection rate until no further change was observed in the oil level of the effluent sample. Figure 12 shows the cumulative oil recovery (% OOIP) from the experiment. Note that the oil recovery has been corrected for the 3-pentanone concentration in the produced oil. The IB injection recovered 56.3% OOIP after 3.48 HCPVI, and the water breakthrough was observed at 0.24 HCPVI. An additional 24.8% OOIP was recovered from the subsequent 6.91 HCPVI of 3pIB for a total of 81.1% OOIP. Figure 12 also shows the concentration of 3-pentanone in the recovered oleic and aqueous phases. 3-Pentanone was not detected in the recovered brine until after 2.4 HCPVI of 3pIB and reached a maximum concentration of 0.276-wt% at the end of the injection, while 3-pentanone was not detected in the recovered oil until after 4.3 HCPVI of 3pIB and reached a maximum concentration of 3.55-wt% at the end of the injection.

These results indicate a substantial delay in the breakthrough time of 3-pentanone, which was observed for the first time in this research. The delayed breakthrough of 3-pentanone can be attributed mainly to the accumulation of 3-pentanone in the oleic and aqueous phases inside the core. That is, 3-pentanone preferentially partitioned into the resident brine (FB and IB) and oil before being produced with the brine and then the oil. Figure 13 shows this accumulation through the accumulated fraction of brine (F_1) and 3-pentanone (F_3). F_1 shows a sharp decrease in F_1 immediately after the water breakthrough and continued to remain below 0.1 throughout the IB injection stage, indicating the inefficient oil recovery after the breakthrough.

During the 3pIB injection stage, F_3 shows an initial accumulation of 3-pentanone on the rock surface and fluid phases. After 5.9 HCPVI, a small amount (0.0097-wt%) of 3-pentanone was produced with the brine. Then, 3-pentanone continued to be produced in both the brine and oil, and F_3 gradually declined to 0.62. The residual oil saturation as remaining oil after 10.4 HCPVI from the tertiary 3pIB injection was 0.10. However, it is likely that the remaining oleic phase in the core was rich in 3-pentanone due to the accumulation of 3-pentanone in the core. If all the retained 3-pentanone in the oleic and aqueous phases inside the core partitioned into the remaining oleic phase with the remaining oil, then the residual oil saturation from the tertiary 3pIB injection would become 0.14. Therefore, it is reasonable to consider that the actual residual saturation as remaining oil of the 3-pentanone-rich phase was between 0.1 and 0.14 for the tertiary 3pIB case.

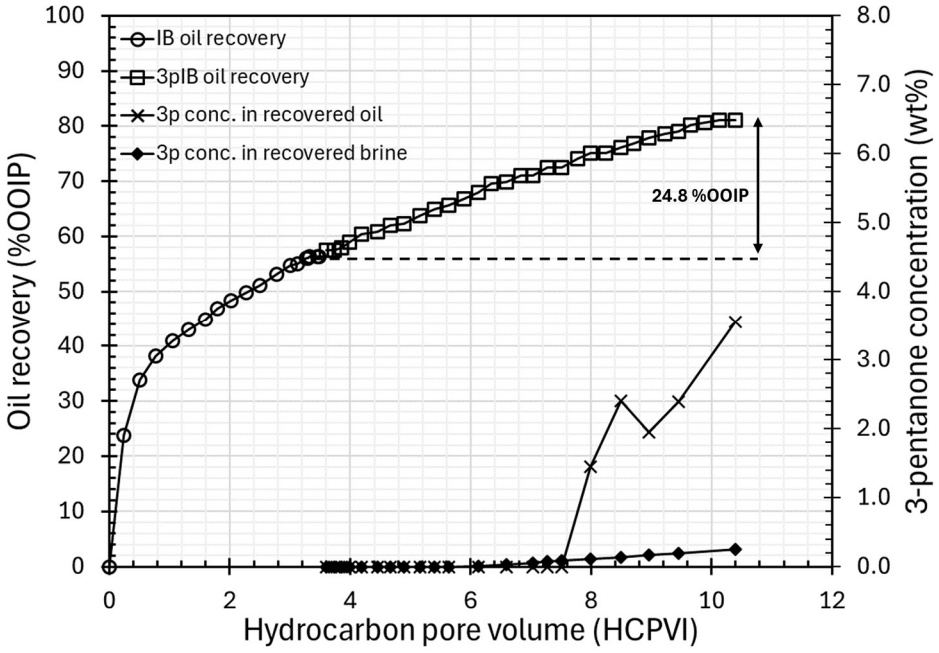

Figure 12—Oil recovery during secondary IB and the subsequent tertiary 3pIB injections.

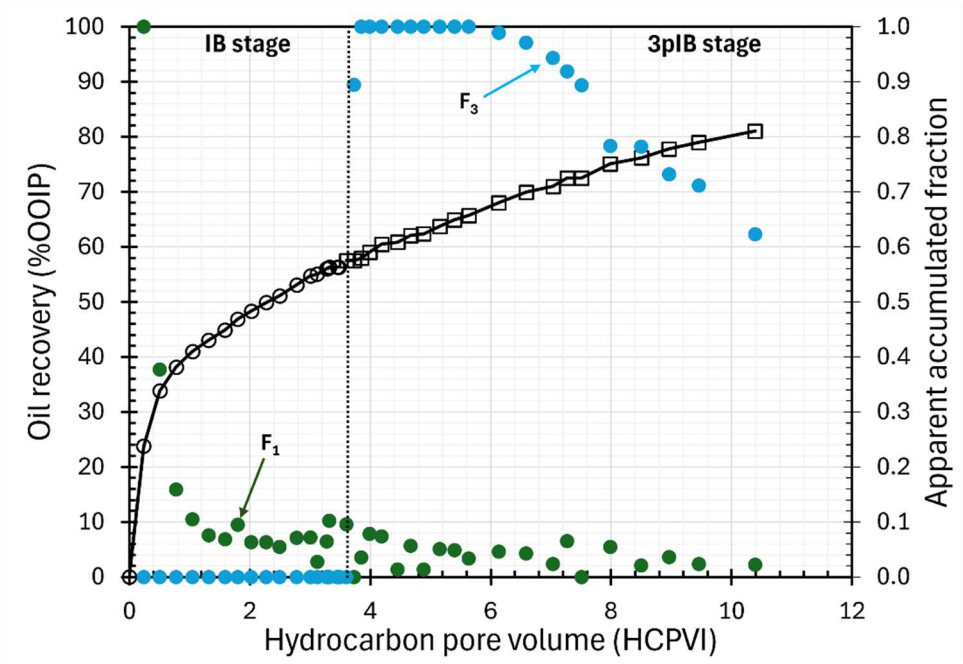

Figure 13—Oil recovery and accumulated fractions of brine and 3-pentanone during secondary IB and the subsequent tertiary 3pIB injections.

Secondary 3pIB Injection.

This coreflood was performed to investigate the performance of 3pIB in the secondary injection mode. After the core preparation, 3pIB was injected for approximately 9.61 HCPV at an injection rate of 5 mL/hr. Figure 14 shows the cumulative oil recovery (% OOIP) from the experiment. The secondary 3pIB injection resulted in 82.8% OOIP after correcting the recovered oil volume for the 3-pentanone concentration in the recovered oil. The water breakthrough time occurred at 0.25 HCPVI, which was the same as that of the secondary IB coreflood. Figure 14 also shows the concentration of 3-pentanone in the recovered oleic phase. The concentration of 3-pentanone in the recovered aqueous phase for the secondary 3pIB injection case was not yet quantitatively measured upon the preparation of this paper. However, this concentration was estimated using the aqueous phase production trend from the tertiary 3pIB injection, assuming that the partitioning behavior of 3-pentanone in both injection schemes was the same.

3-Pentanone was observed in the recovered oil and brine at similar times, after 3.29 HCPVI of 3pIB injection. This similar breakthrough time of 3-pentanone in the produced oil and brine, in contrast with the tertiary 3pIB injection case, is likely because of the absence of a preceding IB injection stage in the secondary 3pIB injection case.

Figure 15 shows the accumulated fraction of brine (F_1) and 3-pentanone (F_3). F_1 shows a sharp decrease in accumulated brine immediately after the water breakthrough and it continued to remain below 0.1 throughout the 3pIB injection. This implies that a large amount of the injected brine was produced along with the oil in the matrix after the water breakthrough. Additionally, F_3 shows an initial adsorption of 3-pentanone on the rock surface and fluid phases in the core before 3-pentanone was then produced in both the brine and oil.

The residual oil saturation as remaining oil from the 9.6 HCPV of secondary 3pIB injection was 0.09. Similar to the tertiary 3pIB injection, it is likely that the remaining oleic phase in the core was rich in 3-pentanone due to the accumulation of 3-pentanone in the core. Similarly, if all the retained 3-pentanone in the oleic and aqueous phases inside the core partitioned into the remaining oleic phase with the remaining oil, the residual oil saturation from the secondary 3pIB injection would become 0.13. This is similar to the value of 0.14 obtained after the tertiary 3pIB injection. Therefore, the actual residual saturation as remaining oil of the 3-pentanone-rich phase after the secondary 3pIB injection should then be between 0.09 and 0.13.

Figure 16 compares the oil recovery histories of the secondary and tertiary 3pIB injection. Although they have similar oil recovery histories until water breakthrough, the secondary 3pIB injection case showed a slightly faster oil recovery than the tertiary 3pIB injection until it reached a plateau at 9.2 HCPV of 3pIB injection.

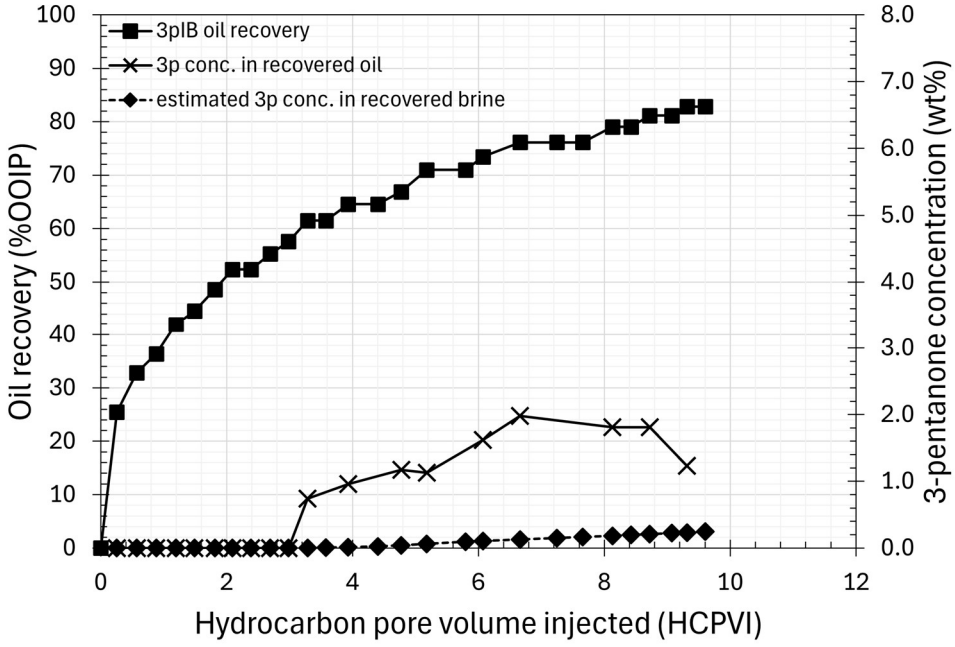

Figure 14—Oil recovery during the secondary 3pIB injection.

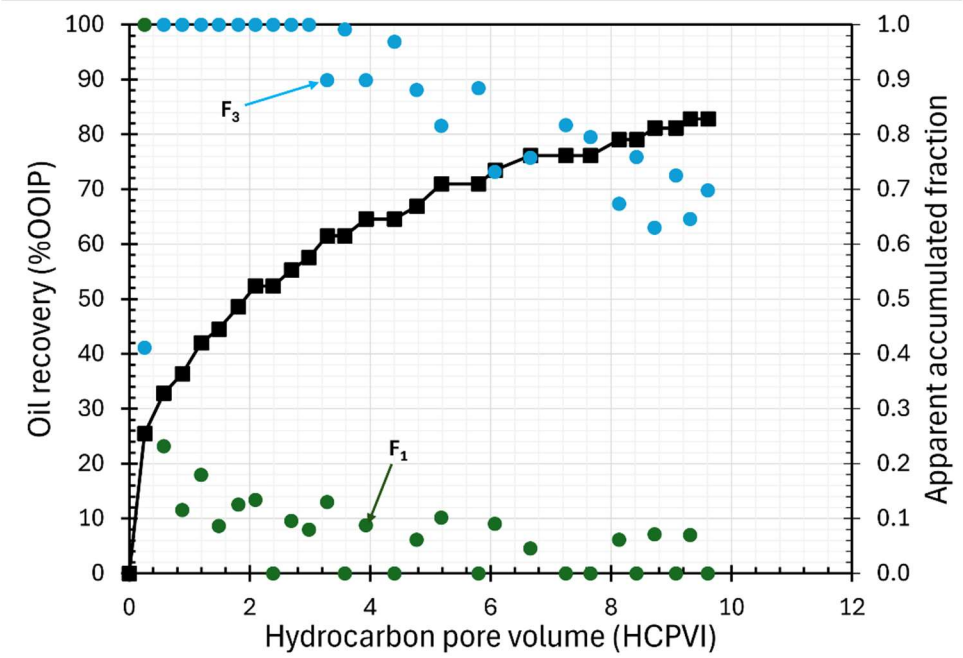

Figure 15—Oil recovery and accumulated fractions of brine and 3-pentanone during the secondary 3pIB injection.

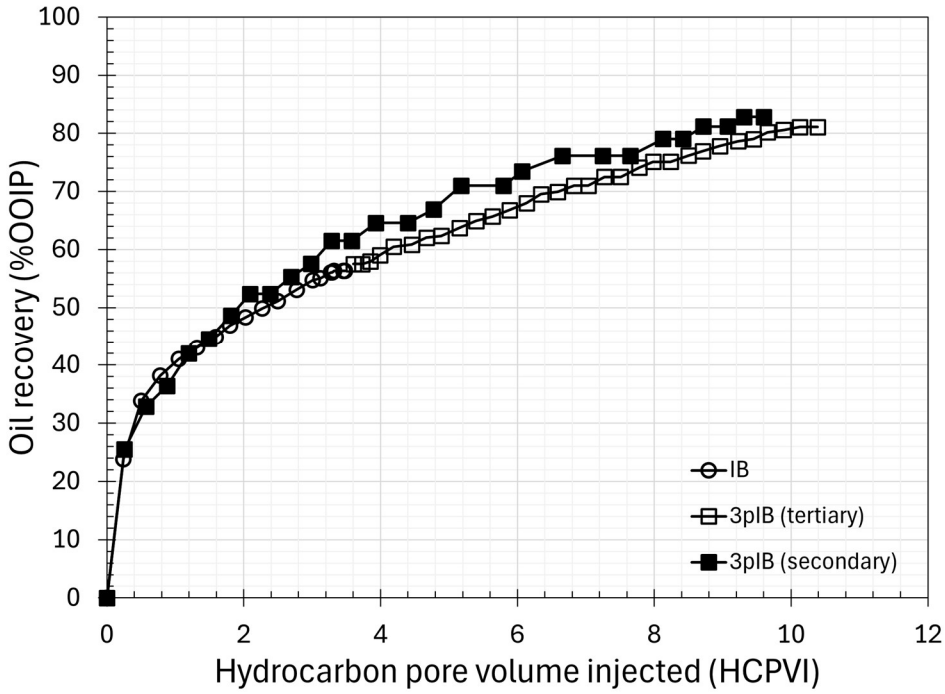

Figure 16—Comparison of oil recoveries by secondary and tertiary 3pIB injections.

Figure 17 shows the normalized oil recoveries with respect to the mass of 3-pentanone injected. The secondary 3pIB case shows a slightly greater efficiency than the tertiary 3pIB case; that is, for a given mass of 3-pentanone injected, the secondary 3pIB case recovered slightly more oil than the tertiary 3pIB case. This can be because the capillary forces in the secondary 3pIB case with a smaller water saturation took advantage of the wettability alteration by 3-pentanone more than in the tertiary 3pIB.

Argüelles-Vivas et al. (2020) studied the impact of initial water saturation on oil recovery by dynamic imbibition experiments using aqueous 3-pentanone solution, in which the sole mechanism of oil recovery was the water imbibition from the fracture volume into the surrounding carbonate matrices with a limited resident time of the injection fluid in the fracture volume. Their results showed the enhancement of water imbibition by 3-pentanone was more pronounced in the presence of initial water in the core, in comparison to no initial water saturation. Further experimental studies are needed to understand the impact of water saturation on ketone EOR.

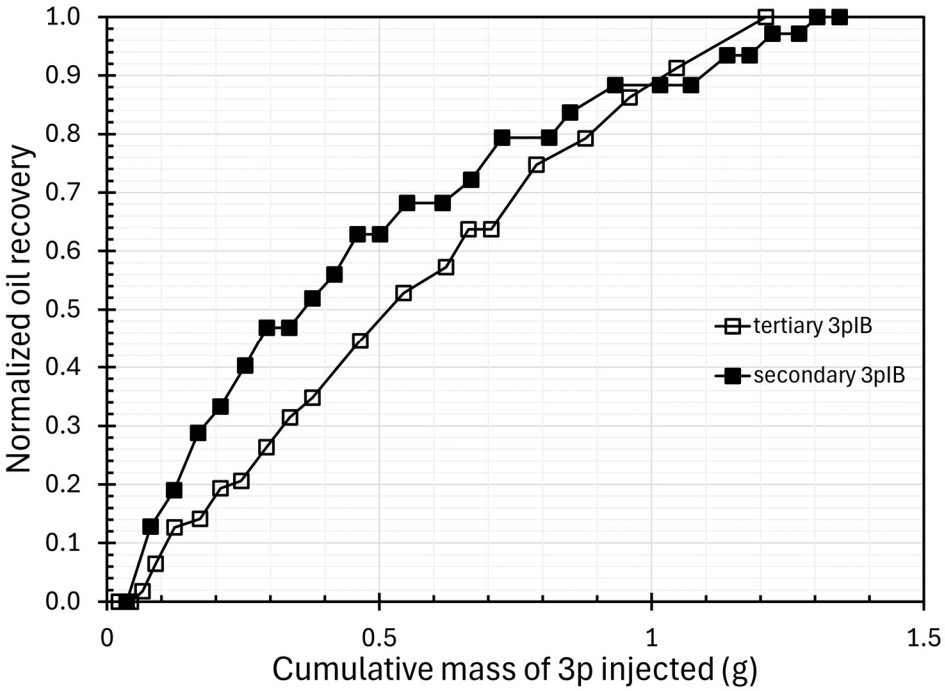

Figure 17—Comparison of oil recoveries by secondary and tertiary 3pIB injections.

The history-matching of the coreflooding data adjusted relative permeability parameters. We simulated the IB injection experiment and the secondary 3pIB injection experiment. The presented results are qualitative because there was a set of uncertain inputs that may have affected the history-matched relative permeability curves. For example, we assumed a 34.5-kPa pressure drop across the core sample because pressure logs were fragmentary. In addition, the residual oil saturation was determined from the history-matching of the experimental data for a finite HCPVI; therefore, it should be regarded as an apparent value. While the measured residual oil saturation to IB and 3pIB from the IB (3.48 HCPVI) and secondary 3pIB injections (9.6 HCPVI) were 24% and 9%, respectively, we used 19% for the former and 6% for the latter in the simulations. Note that matching the experimental data was not possible without reducing the residual oil saturation. Also note that in the simulation of the secondary 3pIB injection, we did not account for the partitioning of 3-pentanone into the in-situ water and oil.

Figure 18 shows the results of the history matching of the IB coreflooding experiment. The obtained relative permeability curves are presented in Figure 19. Figure 20 shows the results of the history matching of the secondary 3pIB coreflooding. The obtained relative permeability curves are displayed in Figure 21. Qualitative assessment of the relative permeability curves reveals a shift toward a more water-wet state during 3pIB injection as this case is associated with a lower water relative permeability curve compared to that of IB. The calculated Lak wettability indices are 0.05 and 0.15 for IB and secondary 3pIB injection cases, respectively, confirming wettability alteration by 3pIB injection. The modified Lak wettability indices are 0.23 and 0.29 for IB and secondary 3pIB injection cases, respectively. The obtained relative permeability curves in the coreflooding experiments are consistently greater than relative permeability curves in the spontaneous imbibition displacements. This agrees with the existing literature (e.g., Bourbiaux and Kalaydjian, 1990) where co-current displacements are associated with greater relative permeabilities than counter-current displacements.

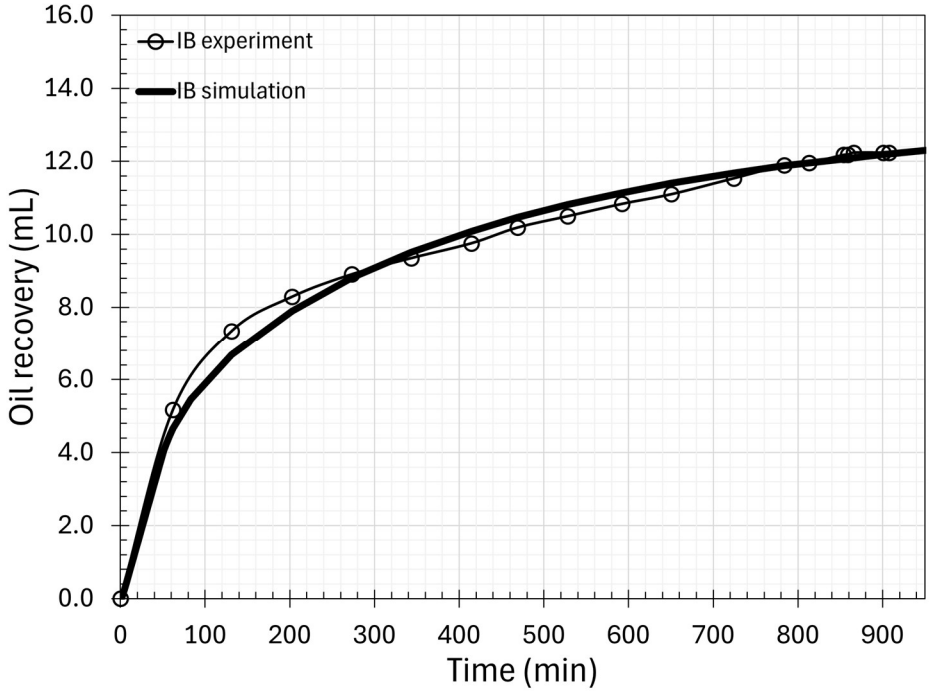

Figure 18—History-matched result of recovered oil volume during the IB coreflood.

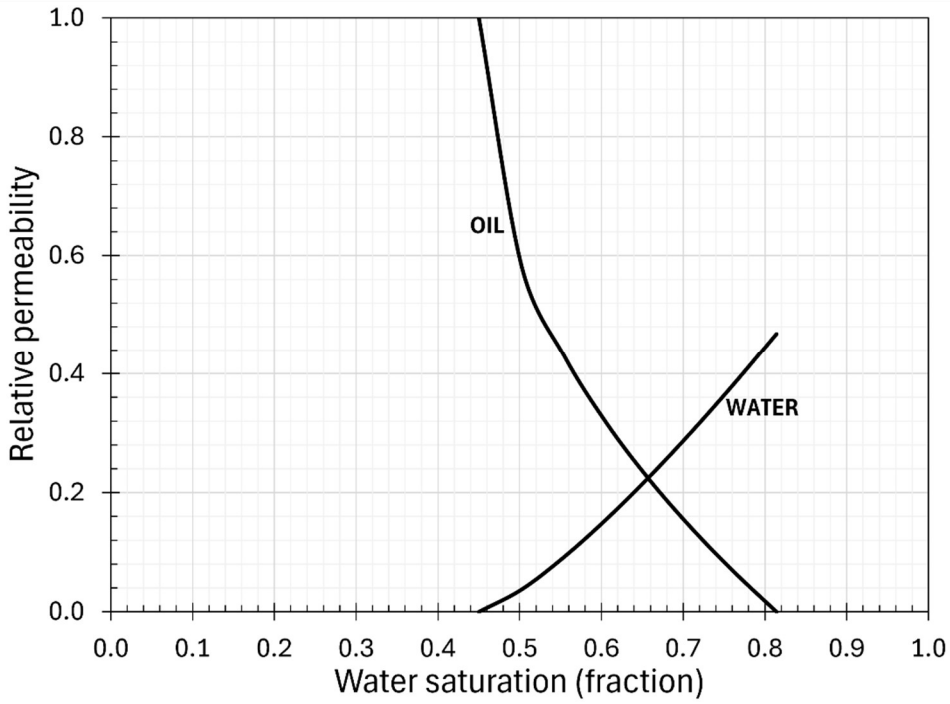

Figure 19—History-matched relative permeability curves for the IB coreflood. Lak and modified Lak wettability indices are 0.05 and 0.23.

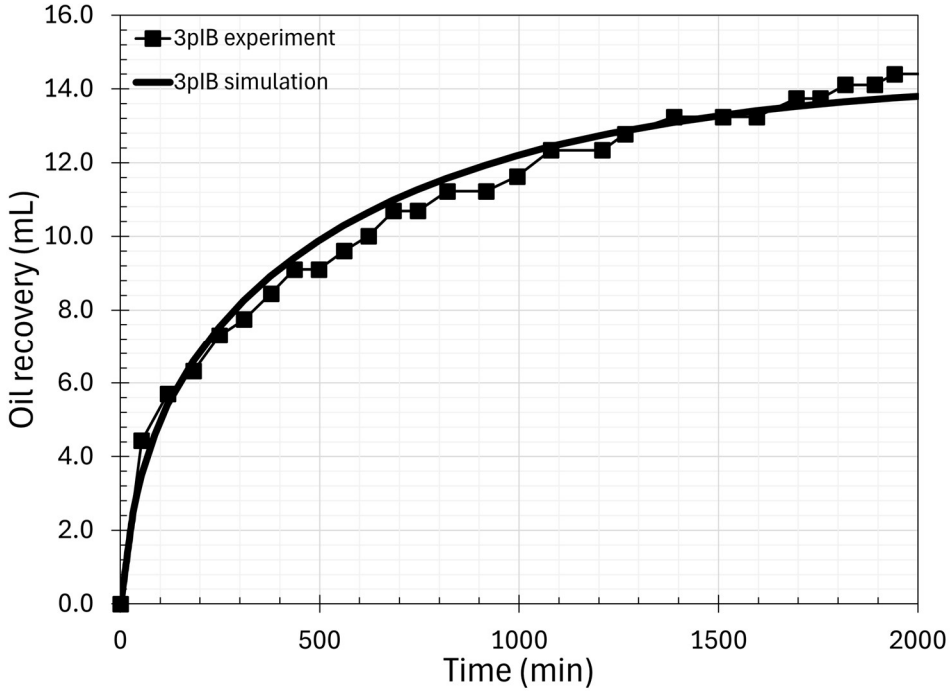

Figure 20—History-matched result of recovered oil volume during secondary 3pIB coreflood.

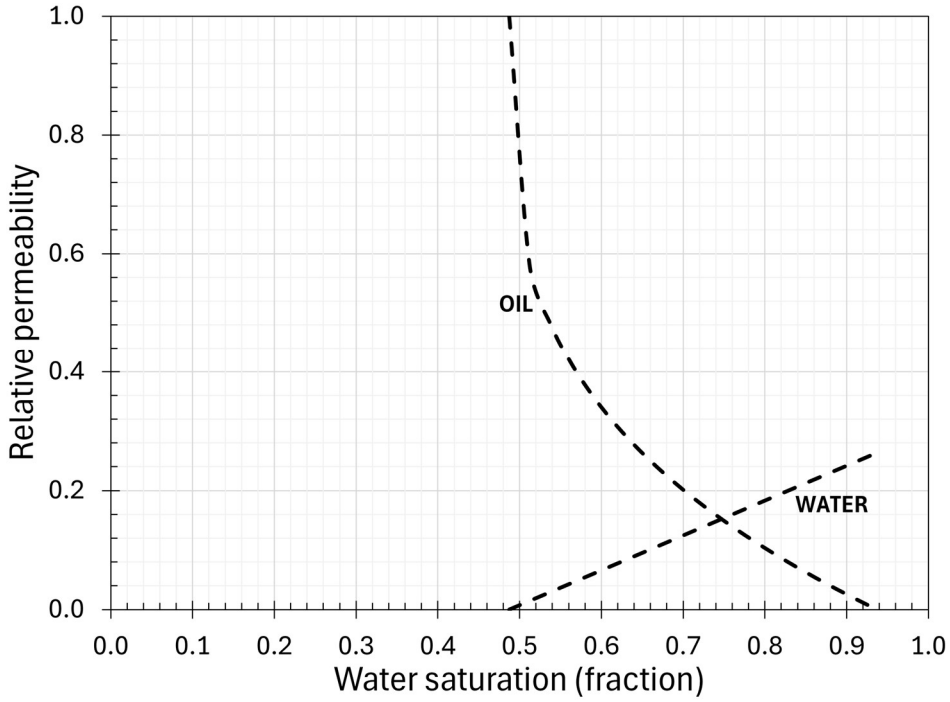

Figure 21—History-matched relative permeability curves for the secondary 3pIB coreflood. Lak and modified Lak wettability indices are 0.15 and 0.29.

4. Conclusions

This paper presented an experimental investigation of aqueous 3-pentanone solution for improved oil recovery in high-salinity high-temperature (HSHT) carbonate reservoirs. Amott wettability tests and secondary and tertiary corefloods were performed on crude-aged Texas Cream limestone cores using injection brine (IB) and 1.1-wt% 3-pentanone in IB (3pIB). The experimental data were history-

matched in a numerical model by adjusting the relative permeability and capillary pressure, which were used to infer the extent of wettability alteration. The main conclusions are as follows:

1. Spontaneous imbibition at 95°C showed that 3pIB led to a more rapid oil recovery compared to IB. The total oil recovery was 34.0% for 3pIB and 24.4% for IB. The subsequent forced displacement resulted in a final oil recovery of 92.4% with 3pIB and 83.3% with IB. The Amott indices to water were 0.37 for 3pIB and 0.29 for IB. The Lak and modified Lak indices were determined by history matching of the spontaneous imbibition data. Results collectively indicated that the addition of 3-pentanone to the injection brine contributed to wettability alteration of the core from an oil-wet state to a more water-wet state. The Lak index was 0.12 for the 3pIB case and 0.03 for the IB case. The modified Lak index was 0.46 for the 3pIB case and 0.45 for the IB case. The spontaneous imbibition rate slope was 0.056 for the 3pIB case and 0.034 for the IB case.

2. Tertiary coreflooding experiments with 3pIB demonstrated its potential to increase oil recovery after initial waterflooding by the IB. The IB recovered 56.3 %OOIP after 3.48 HCPVI, while the 3pIB recovered an additional 24.8 %OOIP after 6.91 PVI. Comparison of the tertiary and secondary coreflooding experiments showed a similar ultimate oil recovery for both injection schemes, although the secondary scheme resulted in a slightly faster oil recovery, recovering a similar amount of oil in 9.6 HCPVI compared to 10.4 PVI in the tertiary scheme. The Lak and modified Lak wettability indices based on the history matching of the coreflooding data indicated wettability alteration of the core from an oil-wet state to a more water-wet state for the 3pIB case than the IB case. The Lak and modified Lak indices were 0.15 and 0.29, respectively, for the 3pIB case, and 0.05 and 0.23 for the IB case.

3. Corefloods with aqueous 3-pentanone solution were performed for the first time in this research. Material balance analysis of the corefloods showed a substantial accumulation of 3-pentanone in the core, resulting in a delayed breakthrough of 3-pentanone. In the tertiary flood, 3-pentanone was not detected in the recovered brine until after 2.4 HCPVI of 3pIB and reached a maximum concentration of 0.276-wt% at the end of the injection. It took 4.3 HCPVI of 3pIB until 3-pentanone was detected in the produced oil, and a maximum concentration of 3.55-wt% occurred at the end of the injection. The substantial accumulation of 3-pentanone in the swept volume can be attributed to the asymmetric solubility of 3-pentanone in high-salinity formation brine (224,358 ppm), 0.3-wt%, and low-salinity injection brine (54,471 ppm), 1.1-wt%, and to the complete miscibility between 3-pentanone and oil. The substantial salinity gradient near the oil-displacement front should have caused the interphase mass transfer of 3-pentanone from the injection brine to the in-situ oil.

Acknowledgments

We gratefully acknowledge the sponsors of the Energi Simulation Industrial Affiliate Program on Carbon Utilization and Storage (ES Carbon UT) at the University of Texas at Austin. Ryosuke Okuno holds the Pioneer Corporation Faculty Fellowship in Petroleum Engineering at the University of Texas at Austin.

References

Al Shalabi, E.W., Sepehrnoori, K., and Delshad, M. 2014. Mechanisms behind Low Salinity Water Injection in Carbonate Reservoirs. *Fuel* **121**(4): 11–19. https://doi.org/10.1016/j.fuel.2013.12.045.

Alammari, F.G., Miller, C.S., and Mohanty, K.K. 2020. Wettability Altering Surfactants for High Temperature Tight Carbonate Reservoirs. Paper presented at the SPE Improved Oil Recovery Conference, Virtual, 31 August – 4 September. SPE-200348-MS. https://doi.org/10.2118/200348-MS.

Alghunaim, E., Uzun, O., Kazemi, H., et al. 2021. Cost-Effective Chemical EOR for Heterogenous Carbonate Reservoirs Using a Ketone-Surfactant System. Paper presented at the SPE Annual Technical Conference and Exhibition, Dubai, UAE, 21 – 23 September. SPE-205910-MS. https://doi.org/10.2118/205910-MS.

Allan, J., and Sun, S.Q. 2003. Controls on Recovery Factor in Fractured Reservoirs: Lessons Learned from 100 Fractured Fields. Paper presented at the SPE Annual Technical Conference and Exhibition, Denver, Colorado, USA, 5 – 8 October. SPE-84590-MS. https://doi.org/10.2118/84590-MS.

Alvarez, J.O., and Schechter, D.S. 2016. Wettability Alteration and Spontaneous Imbibition in Unconventional Liquid Reservoirs by Surfactant Additives. *SPE Reservoir Evaluation & Engineering* **20**(01): 107–17. https://doi.org/10.2118/177057-PA.

Alvarez, J.O., Saputra, I.W., and Schechter, D.S. 2018. The Impact of Surfactant Imbibition and Adsorption for Improving Oil Recovery in the Wolfcamp and Eagle Ford Reservoirs. *SPE Journal* **23**(06): 2103–17. https://doi.org/10.2118/187176-PA.

Argüelles-Vivas, F.J., Wang, M., Abeykoon, G.A., et al. 2020. Oil Recovery from Fractured Porous Media with/without Initial Water Saturation by Using 3-Pentanone and Its Aqueous Solution. *Fuel* **276**: 118031. https://doi.org/10.1016/j.fuel.2020.118031.

Argüelles-Vivas, F.J., Abeykoon, G.A., and Okuno, R. 2022. Chapter 13 - Wettability Modifiers for Enhanced Oil Recovery from Tight and Shale Reservoirs. In *Unconventional Shale Gas Development*, edited by Rouzbeh G. Moghanloo, 345–91. Gulf Professional Publishing. https://doi.org/10.1016/B978-0-323-90185-7.00012-1.

Austad, T., and Milter, J. 1997. Spontaneous Imbibition of Water Into Low Permeable Chalk at Different Wettabilities Using Surfactants. Paper presented at the International Symposium on Oilfield Chemistry, Houston, Texas, USA, 18 – 21 February. SPE-37236-MS. https://doi.org/10.2118/37236-MS.

Barnes, J.R., Smit, J.P., Smit, J.R., et al. 2008. Development of Surfactants for Chemical Flooding at Difficult Reservoir Conditions. Paper presented at the SPE/DOE Improved Oil Recovery Symposium, Tulsa, Oklahoma, USA, 19 – 23 April. SPE-113313-MS. https://doi.org/10.2118/113313-MS.

Belhaj, A.F., Elraies, K.A., Shuhili, J.A., et al. 2020. Surfactant Adsorption Evaluation in the Presence of Crude Oil at High Reservoir Temperature Condition. Paper presented at the Offshore Technology Conference Asia, Virtual, 2 – 6 November. OTC-30141-MS. https://doi.org/10.4043/30141-MS.

Bourbiaux, B.J., and Kalaydjian, F.J. 1990. Experimental Study of Cocurrent and Countercurrent Flows in Natural Porous Media. *SPE Reservoir Engineering* **5**(03): 361–68. https://doi.org/10.2118/18283-PA.

Burrows, L.C., Haeri, F., Cvetic, P., et al. 2020. A Literature Review of CO_2, Natural Gas, and Water-Based Fluids for Enhanced Oil Recovery in Unconventional Reservoirs. *Energy & Fuels* **34**(5): 5331–80. https://doi.org/10.1021/acs.energyfuels.9b03658.

Chen, P., and Mohanty, K.K. 2015. Surfactant-Enhanced Oil Recovery from Fractured Oil-Wet Carbonates: Effects of Low IFT and Wettability Alteration. Paper presented at the SPE International Symposium on Oilfield Chemistry, The Woodlands, Texas, USA, 13 – 15 April. SPE-173797-MS. https://doi.org/10.2118/173797-MS.

Computer Modeling Group, 2020. STARS Version 2018 User's Guide. Computer Modelling Group, Calgary, Alberta, Canada.

Gbadamosi, A.O., Junin, R., Manan, M.A., et al. 2019. An Overview of Chemical Enhanced Oil Recovery: Recent Advances and Prospects. *International Nano Letters* **9**(3): 171–202. https://doi.org/10.1007/s40089-019-0272-8.

Kathel, P., and Mohanty, K.K. 2013. Wettability Alteration in a Tight Oil Reservoir. *Energy & Fuels* **27**(11): 6460–68. https://doi.org/10.1021/ef4012752.

Kulkarni, R. D., and Somasundaran, P. 1976. Mineralogical heterogeneity of ore particles and its effects on their interfacial characteristics. *Powder Technology* **14**(2): 279-285.

Lake, L., Johns, R.T., Rossen, W.R., et al. 2014. *Fundamentals of Enhanced Oil Recovery*. https://doi.org/10.2118/9781613993286.

Lawal, T., Wang, M., Abeykoon, G.A., et al. 2022. Effect of Chemical Partition Behavior on Oil Recovery by Wettability Alteration in Fractured Tight Reservoirs. *Energy & Fuels* **36**(2): 797–805. https://doi.org/10.1021/acs.energyfuels.1c03344.

Levitt, D., Klimenko, A., Jouenne, S., et al. 2016. Designing and Injecting a Chemical Formulation for a Successful Off-Shore Chemical EOR Pilot in a High-Temperature, High-Salinity, Low-Permeability Carbonate Field. Paper presented at the SPE Improved Oil Recovery Conference, Tulsa, Oklahoma, USA, 11 – 13 April. SPE-179679-MS. https://doi.org/10.2118/179679-MS.

Lu, Y., Najafabadi, N.F., and Firoozabadi, A. 2019. Effect of Low-Concentration of 1-Pentanol on the Wettability of Petroleum Fluid–Brine–Rock Systems. *Langmuir* **35**(12): 4263–69. https://doi.org/10.1021/acs.langmuir.9b00099.

Manrique, E.J., Engineering, N.Q., and Muci, V.E. 2007. EOR Field Experiences in Carbonate Reservoirs in the United States. *SPE Res Eval & Eng* **10**(06): 667-686. https://doi.org/10.2118/100063-PA.

McCaffery, F.G., and Mungan, N. 1970. Contact Angle And Interfacial Tension Studies of Some Hydrocarbon-Water-Solid Systems. *Journal of Canadian Petroleum Technology* **9**(03). https://doi.org/10.2118/70-03-04.

Mirzaei-Paiaman, A., Masihi, M., and Standnes, D.C. 2013. Index for Characterizing Wettability of Reservoir Rocks Based on Spontaneous Imbibition Recovery Data. *Energy & Fuels* **27**(12): 7360–68. https://doi.org/10.1021/ef401953b.

Mirzaei-Paiaman, A., Saboorian-Jooybari, H., and Masihi, M. 2017. Incorporation of Viscosity Scaling Group into Analysis of MPMS Index for Laboratory Characterization of Wettability of Reservoir Rocks. *Journal of Petroleum Exploration and Production Technology* **7**(1): 205–16. https://doi.org/10.1007/s13202-016-0231-0.

Mirzaei-Paiaman, A. 2021. New Methods for Qualitative and Quantitative Determination of Wettability from Relative Permeability Curves: Revisiting Craig's Rules of Thumb and Introducing Lak Wettability Index. *Fuel* **288**: 119623. https://doi.org/10.1016/j.fuel.2020.119623.

Mirzaei-Paiaman, A., Faramarzi-Palangar, M., Djezzar, S., et al. 2022. A New Approach to Measure Wettability by Relative Permeability Measurements. *Journal of Petroleum Science and Engineering* **208**: 109191. https://doi.org/10.1016/j.petrol.2021.109191.

Morsy, S., Sheng, J.J., and Soliman, M.Y. 2013. Waterflooding in the Eagle Ford Shale Formation: Experimental and Simulation Study. Paper presented at the SPE Unconventional Resources Conference and Exhibition-Asia Pacific, Brisbane, Australia, 11 – 13 November. SPE-167056-MS. https://doi.org/10.2118/167056-MS.

Puerto, M., Hirasaki, G.J., Miller, C. A., Barnes, J. R. 2012. Surfactant Systems for EOR in High-Temperature, High-Salinity Environments. *SPE J* **17**(01): 11-19. https://doi.org/10.2118/129675-PA.

Sheng, J.J. 2013. Comparison of the Effects of Wettability Alteration and IFT Reduction on Oil Recovery in Carbonate Reservoirs. *Asia-Pacific Journal of Chemical Engineering* **8**(1): 154–61. https://doi.org/10.1002/apj.1640.

Sheng, J.J. 2015. Status of Surfactant EOR Technology. *Petroleum* **1**(2): 97–105. https://doi.org/10.1016/j.petlm.2015.07.003.

Somasundaran, P., and Fuerstenau, D. W. 1973. Heat and entropy of adsorption and association of long-chain surfactants at the alumina-aqueous solution interface. *Transactions*, 254.

Standnes, D.C., and Austad, T. 2000. Wettability Alteration in Chalk: 2. Mechanism for Wettability Alteration from Oil-Wet to Water-Wet Using Surfactants. *Journal of Petroleum Science and Engineering* **28**(3): 123–43. https://doi.org/10.1016/S0920-4105(00)00084-X.

Wang, M., Abeykoon, G.A., Argüelles-Vivas, F.J., et al. 2019. Ketone Solvent as a Wettability Modifier for Improved Oil Recovery from Oil-Wet Porous Media. *Fuel* **258**: 116195. https://doi.org/10.1016/j.fuel.2019.116195.

Wang, M., Baek, K.H., Abeykoon, G.A., et al. 2020. Comparative Study of Ketone and Surfactant for Enhancement of Water Imbibition in Fractured Porous Media. *Energy & Fuels* **34**(5): 5159–67. https://doi.org/10.1021/acs.energyfuels.9b03571.

Wang, M., Abeykoon, G.A., Argüelles-Vivas, F.J., et al. 2020. Aqueous Solution of Ketone Solvent for Enhanced Water Imbibition in Fractured Carbonate Reservoirs. *SPE Journal* **25**(05): 2694–2709. https://doi.org/10.2118/200340-PA.

Wang, M., Argüelles-Vivas, F.J., Abeykoon, G.A., et al. 2021. The Effect of Initial Water Saturation on Enhanced Water Imbibition by Surfactant for Fractured Tight Porous Media. *SPE Journal* **26**(02): 847–56. https://doi.org/10.2118/200431-PA.

Wang, M., Abeykoon, G.A., Argüelles-Vivas, F.J., et al. 2022. Aqueous Solution of 3-Pentanone for Enhanced Oil Production from Tight Porous Media. *Journal of Petroleum Science and Engineering* **213**: 110376. https://doi.org/10.1016/j.petrol.2022.110376.

Zeng, T., S. Miller, C., and Mohanty, K. 2018. Application of Surfactants in Shale Chemical EOR at High Temperatures. Paper presented at the SPE Improved Oil Recovery Conference, Tulsa, Oklahoma, USA, 14 – 18 April. SPE-190318-MS. https://doi.org/10.2118/190318-MS.

Ziegler, V.M., and Handy, L.L. 1981. Effect of Temperature on Surfactant Adsorption in Porous Media. *Society of Petroleum Engineers Journal* **21**(02): 218–28. https://doi.org/10.2118/8264-PA.